Available online at www.sciencedirect.com
ScienceDirect
Ceramics International 37 (2011) 2263–2267
CERAMICS INTERNATIONAL
www.elsevier.com/locate/ceramint

Effects of ball milling and post-annealing on the transparency of spark plasma sintered Lu_2O_3

Liqiong An, Akihiko Ito, Takashi Goto *

Institute for Materials Research, Tohoku University, 2-1-1 Katahira, Aoba-ku, Sendai 980-8577, Japan

Received 28 January 2011; received in revised form 4 March 2011; accepted 8 March 2011
Available online 16 March 2011

Abstract

The effects of ball milling of starting powder and post-annealing of spark plasma sintered (SPSed) Lu_2O_3 on its microstructure and optical property were investigated. When ball-milled powder was used, the SPSed Lu_2O_3 was found to have a larger grain size with wider distribution and lower transparency than in the case using powder without ball milling. After annealing at 1323 K in air, the Lu_2O_3 that was SPSed using ball-milled powder became colorless, had a higher transmittance in the visible spectrum than the case where as-received powder was used, and exhibited transmittances of 71.4% and 81.6% for wavelengths of 550 and 2000 nm, respectively.

Keywords: Transparent ceramics; Lutetium oxide; Ball milling; Spark plasma sintering

1. Introduction

Polycrystalline transparent ceramics have attracted much attention owing to their many applications, including gain media for solid-state lasers [1], envelopes for high-intensity discharge lamps [2], and windows and domes for infrared sensors [3]. Optically transparent ceramics have been fabricated by pressureless sintering in a vacuum or hydrogen (H_2) atmosphere. The grain size of a sintered body produced by pressureless sintering usually exceeds several or hundreds of micrometers because of the high sintering temperature and long holding time. This results in a deterioration of its mechanical properties. Spark plasma sintering (SPS) is a promising method that can be used in the fabrication of high-density ceramics having fine grains at a relatively low temperature and within a short holding time. By carefully controlling the SPS conditions, highly transparent ceramics can be fabricated [4,5].

Lutetium oxide (Lu_2O_3) is a promising transparent ceramic material that has various optical applications owing to its high mechanical properties, good chemical stability, and high thermal conductivity [6]. Transparent Lu_2O_3 has been fabricated using different starting powders, mainly homemade nano-sized powders. Zych et al. reported transparent Eu:Lu_2O_3 using powder synthesized by a combustion method [7]. Transparent Nd:Lu_2O_3 using powders synthesized by a co-precipitation method was reported by Lu et al. [8] and Chen et al. [9]. Although these homemade powders are highly sinterable and yield superior transparency, commercially available powder is more useful for a wider range of practical applications. We have previously reported the preparation of transparent Lu_2O_3 using commercial powder by SPS [10]. However, the sintered Lu_2O_3 body was slightly colored. Pre-treatment of the source powder and post-annealing of the sintered body can be effective in improving the transparency of a SPSed Lu_2O_3 body. In this study, we investigated the effects of ball milling of commercial powder and post-annealing of SPSed Lu_2O_3 on its microstructure and optical properties.

2. Experimental procedure

Commercial Lu_2O_3 powder (Kojundo Chemical Lab, Japan; purity: 99.9%) was used. The as-received powder was pre-treated by ball-milling with a small amount of ethanol and zirconia balls for 12 h. The milled slurry was dried at 333 K in an oven for 24 h, and then ground and sieved through a 200-mesh grid. For comparison, both the as-received and ball-milled powders were sintered using an SPS apparatus (SPS-210

* Corresponding author. Tel.: +81 22 215 2106; fax: +81 22 215 2107.
E-mail address: goto@imr.tohoku.ac.jp (T. Goto).

0272-8842/$36.00
doi:10.1016/j.ceramint.2011.03.017

LX, SPS SYNTEX INC., Japan). The sintering temperature was increased to 873 K within 180 s and then to 1373 K within a further 300 s. This temperature was then maintained for 300 s. The sintering temperature was subsequently increased further to 1723 K at a heating rate of 0.17 K s^{-1}. The sintering temperature was then kept at 1723 K for 2.7 ks. A pressure of 10 MPa was pre-loaded at room temperature, and a final pressure of 100 MPa was loaded above 1373 K and maintained until the end of the sintering procedure. The linear shrinkage of the specimens during the SPS process was continuously monitored by observing the displacement of the punch rod and corrected by the thermal expansion or contraction of the punch rods. The SPSed specimens were mirror-polished on both sides using diamond slurry. The final thickness of the specimens was approximately 1 mm. The specimens were annealed in air at 1323 K for 43.2 ks.

The density was measured using the Archimedes method in distilled water. The specimens were thermally etched in air at 1573 K for 3.6 ks. The microstructure was observed using a field emission scanning electron microscope (FESEM, JSM-7500F, JEOL, Japan). The average grain size was determined from the linear intercept length [11], and the in-line transmittance was measured using a spectrophotometer (UV-3101PC, Shimadzu, Japan) for wavelengths between 190 and 2500 nm, and with a Fourier transform infrared spectrometer (FTIR, 460 Plus, Jasco, Japan) between 4000 and 400 cm^{-1} (2.5–25 μm).

3. Results and discussion

Fig. 1 shows FESEM images of (a) as-received and (b) ball-milled Lu_2O_3 powder. The as-received powder was scaly with an average particle size of 5.55 μm (Fig. 1 (a)). After ball milling, the particles became more homogenous and their average diameter was reduced to about 0.29 μm (Fig. 1(b)).

Fig. 2 shows the sintering curves acquired during the SPS process using as-received and ball-milled powders. Although the final relative density of the Lu_2O_3 that was SPSed using both powders was almost the same (more than 99.5% of the theoretical value), the densification process was affected by the powders. The starting packing density for ball-milled powder was 39.0%, which is slightly greater than the 37.6% that was calculated for as-received powder. At the point where the final pressure was applied (dashed line), the Lu_2O_3 that was SPSed using ball-milled powder had a relative density of 55.4%, whereas that using as-received powder was 52.0%. The increase in relative density may be attributed to a decrease in particle size and the improvement in the flowability of the raw material after ball milling (Fig. 1(b)) [12]. After the pressure was increased to 100 MPa, the relative density of the Lu_2O_3 that was SPSed using as-received powder increased and the densification process finished more quickly than when ball-milled powder was used.

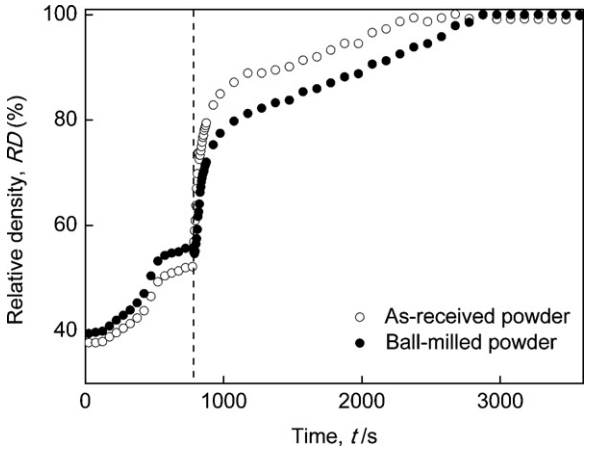

Fig. 2. Sintering curves of Lu_2O_3 sintered by SPS at 1723 K for 2.7 ks using as-received and ball-milled powders. The dashed line refers to the application of final pressure.

Fig. 3 depicts the microstructure and grain size distribution of SPSed Lu_2O_3 using as-received and ball-milled powders. The Lu_2O_3 that was SPSed using as-received powder had an average grain size of 0.68 ± 0.05 μm (0.05 μm: standard deviation, Fig. 3(c)), while that using ball-milled powder was 0.91 ± 0.14 μm (Fig. 3(d)). In the Lu_2O_3 that was SPSed using ball-milled powder, there were larger grains having a wider size distribution than when as-received powder was used.

Fig. 4 presents photographs of Lu_2O_3 that was SPSed using both as-received and ball-milled powders. The lines of text, which were placed 30 mm below the specimens, were legible, and in both cases, were slightly gray in color. The color of the ball-milled powder was a little darker. Fig. 5 shows the transmittance spectra of both specimens in the visible and infrared ranges. As shown in Fig. 5(a), the transmittance increased with wavelength from 275 to 2500 nm, and for the Lu_2O_3 that was SPSed using as-received powder, it was higher

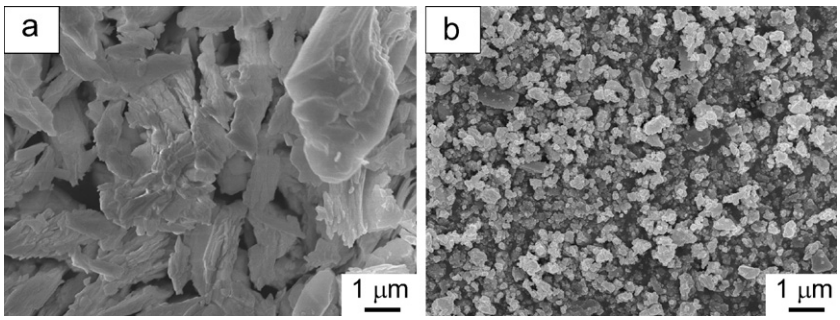

Fig. 1. FESEM images of (a) as-received Lu_2O_3 powder and (b) ball-milled Lu_2O_3 powder.

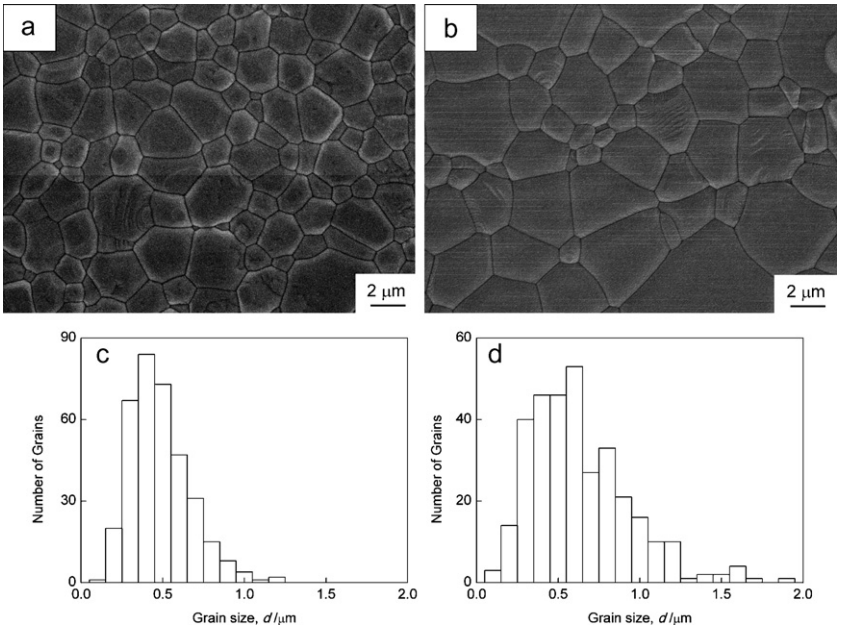

Fig. 3. Microstructure and grain size distribution of Lu_2O_3 SPSed using (a, c) as-received powder and (b, d) ball-milled powder.

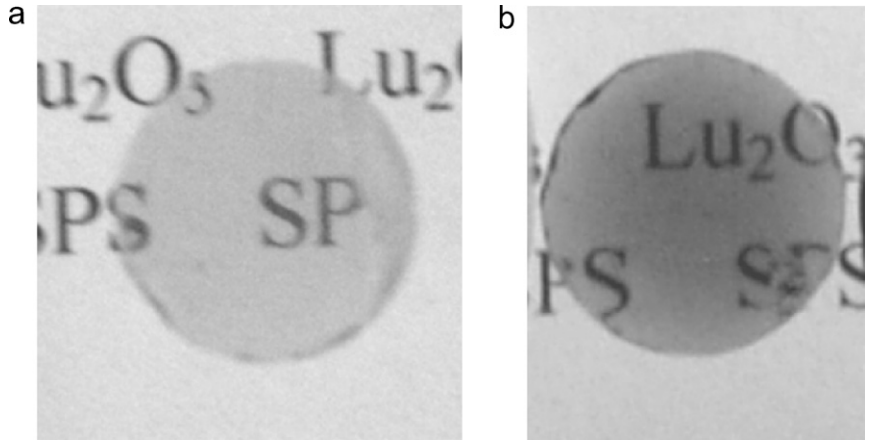

Fig. 4. Photographs of Lu_2O_3 bodies SPSed using (a) as-received powder and (b) ball-milled powder. The bodies were placed 30 mm above the text.

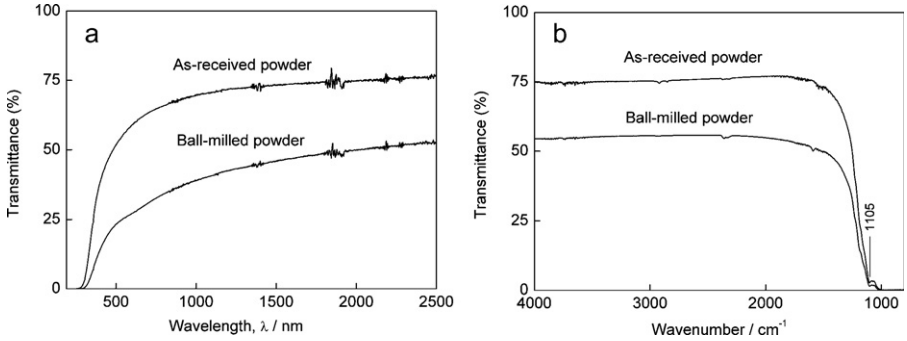

Fig. 5. Transmittance spectra of transparent Lu_2O_3 sintered at 1723 K for 2.7 ks using as-received and ball-milled powders in the ranges (a) 190–2500 nm and (b) 2.5–12.5 μm (4000–800 cm^{-1}).

than the case when ball-milled powder was used. The refractive index of Lu_2O_3 is reported to be 1.90 at 2000 nm [13] and thus the theoretical transmittance can be calculated as 82.5%. The transmittance of the Lu_2O_3 that was SPSed using as-received powder approached 75%, which exceeds 90% of the theoretical value. Weak absorption peaks that were located at 1105 cm^{-1} in both specimens may be associated with C–O–C stretching. Since SPS uses a graphite die, the sintering atmosphere may contain CO and CO_2 gases, and these gases may have been trapped in the specimens.

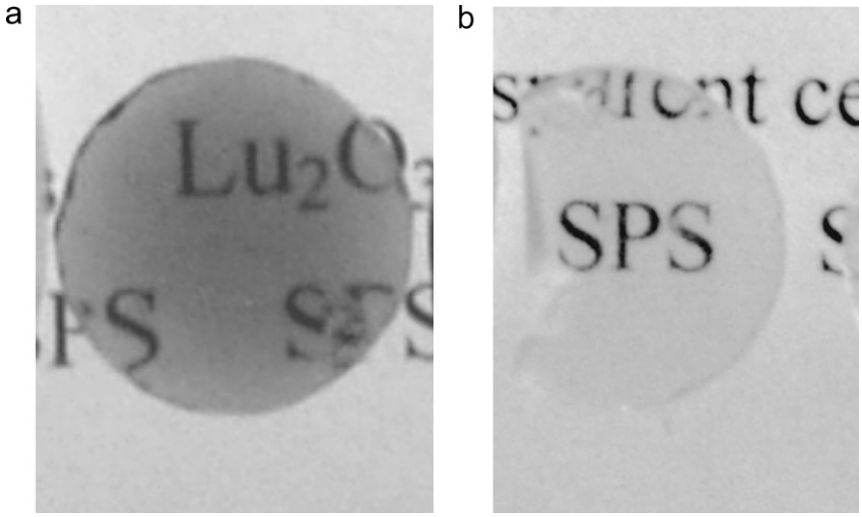

Fig. 6. Photographs of SPSed Lu_2O_3 bodies (a) without annealing and (b) annealed at 1323 K for 43.2 ks using ball-milled powder. The bodies were placed 30 mm above the text.

In general, residual pores and defects can be the main scattering and absorption centers in transparent ceramics. As shown in Fig. 3, pores were rarely observed in the thermally etched surfaces. Defects, particularly oxide vacancies, would form because of the reduced atmosphere during the SPS process, resulting in a darkened, gray appearance [14]. A high concentration of defects may be assumed to be present in the specimen using ball-milled powder because of surface defect formation during the ball milling process [15]. A high concentration of defects may also have caused the gray color [4]. Moreover, the defects would accelerate the grain growth during sintering [16].

Fig. 6 shows photographs of Lu_2O_3 that was SPSed using ball-milled powder before and after annealing in air at 1323 K for 43.2 ks. The color disappeared and the specimen became colorless after annealing. Fig. 7 shows the transmittance spectra of the annealed Lu_2O_3 that was SPSed using different starting powders. When SPSed with either as-received or ball-milled powders, the post-annealing transmittance of the Lu_2O_3 increased significantly over the entire spectrum. For example, the transmittance of Lu_2O_3 that was SPSed using ball-milled powder increased from 25.5% to 71.5% at a wavelength of 550 nm and also increased from 50.0% to 81.6% at a wavelength of 2000 nm. When using ball-milled powder, the corresponding transmittance in the visible spectrum from 230 to 830 nm was higher than when using as-received powder. The weak absorption peak that is located at 1105 cm^{-1} remained in both specimens post-annealing. Two additional peaks appeared at 1514 and 1412 cm^{-1}, which was in agreement with the case of Lu_2O_3 powder and may have been due to C–O stretching [17]. Both of these absorption peaks were more intense in the Lu_2O_3 that was SPSed using ball-milled powder than the case when as-received powder was used. CO and CO_2 gases would have been readily trapped at pores in the non-uniform microstructure of the Lu_2O_3 that was SPSed using ball-milled powder. The ultra-violet absorption edge began at 270 nm for Lu_2O_3 that was SPSed without annealing (Fig. 5(a)) and was 230 nm for those annealed at 1323 K (Fig. 7(a)). The blue-shift of the absorption edge implied that there was a decrease in the number of oxide vacancies [18]. During the annealing process, oxide vacancy was compensated, resulting in its colorlessness and also enhancing its transparency, particularly in the visible range using ball-milled powder.

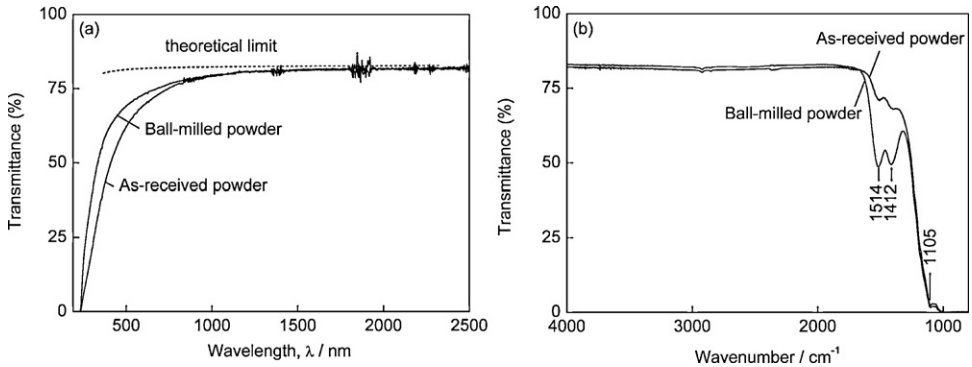

Fig. 7. Transmittance spectra of Lu_2O_3 bodies SPSed using as-received and ball-milled powder after annealing at 1323 K for 43.2 ks in the ranges (a) 190–2500 nm and (b) 2.5–12.5 μm (4000–800 cm^{-1}). Both specimens were sintered at 1723 K for 2.7 ks. The dashed line refers to the theoretical limit in transmittance.

4. Conclusions

The result of ball milling was the formation of small and homogeneous particles. The Lu_2O_3 that was SPSed using ball-milled powder exhibited a larger grain size having wider distribution and lower transmittance than that using as-received powder. After annealing at 1323 K for 43.2 ks, the color of the Lu_2O_3 that was SPSed using both as-received and ball-milled powder disappeared and the transmittance was enhanced. The Lu_2O_3 that was SPSed using ball-milled powder showed higher transmittance in the visible range than that using as-received powder after annealing. The highest transmittance of Lu_2O_3 that was SPSed was 81.6% at a wavelength of 2000 nm.

Acknowledgments

This research was supported in part by the Research Fellowships of the Japan Society for the Promotion of Science for Young Scientists, and by the Global COE Program of Materials Integration, Tohoku University.

References

[1] A. Ikesue, Y.L. Aung, Ceramic laser materials, Nat. Photon. 2 (12) (2008) 721–727.
[2] G.C. Wei, Transparent ceramic lamp envelope materials, J. Phys. D: Appl. Phys. 38 (17) (2005) 3057.
[3] A. Krell, J. Klimke, T. Hutzler, Advanced spinel and sub-μm Al_2O_3 for transparent armour applications, J. Eur. Ceram. Soc. 29 (2) (2009) 275–281.
[4] C. Wang, Z. Zhao, Transparent $MgAl_2O_4$ ceramic produced by spark plasma sintering, Scripta Mater. 61 (2) (2009) 193–196.
[5] B.-N. Kim, K. Hiraga, K. Morita, H. Yoshida, Effects of heating rate on microstructure and transparency of spark-plasma-sintered alumina, J. Eur. Ceram. Soc. 29 (2) (2009) 323–327.
[6] U. Griebner, V. Petrov, K. Petermann, V. Peters, Passively mode-locked Yb:Lu_2O3 laser, Opt. Express 12 (14) (2004) 3125–3130.
[7] E. Zych, J. Trojan-Piegza, P. Dorenbos, Radioluminescence of Lu_2O_3:Eu nanocrystalline powder and vacuum-sintered ceramic, Radiat. Meas. 38 (4–6) (2004) 471–474.
[8] J. Lu, K. Takaichi, T. Uematsu, A. Shirakawa, M. Musha, K. Ueda, H. Yagi, T. Yanagitani, A.A. Kaminskii, Promising ceramic laser material: highly transparent Nd^{3+}:Lu_2O_3 ceramic, Appl. Phys. Lett. 81 (23) (2002) 4324–4326.
[9] Q. Chen, Y. Shi, L. An, J. Chen, J. Shi, Fabrication and photoluminescence characteristics of Eu^{3+}-doped Lu_2O_3 transparent ceramics, J. Am. Ceram. Soc. 89 (6) (2006) 2038–2042.
[10] L. An, A. Ito, T. Goto, Fabrication of transparent lutetium oxide by spark plasma sintering, J. Am. Ceram. Soc. 94 (3) (2011) 695–698.
[11] M.I. Mendelson, Average grain size in polycrystalline ceramics, J. Am. Ceram. Soc. 52 (8) (1969) 443–446.
[12] H. Yoshida, K. Morita, B.-N. Kim, K. Hiraga, M. Kodo, K. Soga, T. Yamamoto, Densification of nanocrystalline yttria by low temperature spark plasma intering, J. Am. Ceram. Soc. 91 (5) (2008) 1707–1710.
[13] A.A. Kaminskii, M.S. Akchurin, P. Becker, K. Ueda, L. Bohatý, A. Shirakawa, M. Takurakawa, K. Takaichi, H. Yagi, J. Dong, T. Yanagitani, Mechanical and optical properties of Lu_2O_3 host-ceramics for Ln^{3+} lasants, Laser Phys. Lett. 5 (4) (2008) 300–303.
[14] D. Jiang, D.M. Hulbert, U. Anselmi-Tamburini, T. Ng, D. Land, A.K. Mukherjee, Optically transparent polycrystalline Al_2O_3 produced by spark plasma sintering, J. Am. Ceram. Soc. 91 (1) (2008) 151–154.
[15] Z. Kóya, I. Vesselenyi, K. Niesz, A. Kukovecz, A. Demortier, A. Fonseca, J. Delhalle, Z. Mekhalif, J.B. Nagy, A.A. Koó, Z. Osváh, A. Kocsonya, L.P. Bir, I. Kiricsi, Large scale production of short functionalized carbon nanotubes, Chem. Phys. Lett. 360 (5–6) (2002) 429–435.
[16] N. Murayama, W. Shin, Effect of rapid heating on densification and grain growth in hot pressed alumina, J. Ceram. Soc. Jpn. 108 (9) (2000) 799–802.
[17] D. Zhou, Y. Shi, J. Xie, Y. Ren, P. Yun, Fabrication and luminescent properties of Nd^{3+}-doped Lu_2O_3 transparent ceramics by pressureless sintering, J. Am. Ceram. Soc. 92 (10) (2009) 2182–2187.
[18] X. He, K. Li, M. Liu, Y. He, X. Zhang, Y. Zhao, D. Xue, An optical spectroscopy study of defects in lithium tantalate single crystals, Opt. Commun. 281 (9) (2008) 2531–2534.